Supporting Information

Preparation, characterization, and energy simulation of $ZnTiO_3$ high near-infrared reflection pigment and its anti-graffiti coating

Song Wang, Jihu Wang *, Shaoguo Wen, Hui Li, Chen Xie, Shuaibiao Li, Dajiang Mei

College of Chemistry and Chemical Engineering, Shanghai University of Engineering Science, Shanghai 201620, PR China
*Correspondence: wangjihu@163.com

S1 Supplemental Experimental Procedure S1: Characterization of Bandgap

Based on the diffuse reflectance spectrum of the powder obtained by the UV-Vis spectrophotometer, the absorption edge and the corresponding band gap of the pigment powder can be calculated by the Kubelka-Munk and Tauc function[1]:

$$F(R) = a = \frac{(1-R)^2}{2R} \quad (1)$$

$$(\alpha h\nu)^{\frac{1}{n}} = A(h\nu - Eg) \quad (2)$$

$$E_g = \frac{1240}{\lambda} \quad (3)$$

where R is the reflectivity of the powder, F(R) is the Kubelka-Munk function and α is absorption coefficients. λ is the wavelength.

Extrapolating the linear region of these plots to [F(R) hv] n = 0 reveals the band gap of the material. In layman's terms, with $X = \frac{1240}{\lambda}$, $Y = \left(F(R) * \frac{1240}{\lambda}\right)^{0.5}$, find the intersection of the tangent of the curve and the x-axis as E_g The obtained band gap is 3.46.

The mean grain size depends on the Scherrer equation for the XRD peak profile:

$$D = \frac{0.89\lambda}{\beta\cos\theta} \quad (4)$$

Where λ is the wavelength of the x-ray, which is 0.154178 nm, θ is the Bragg angle, and β is the half-peak width. The average crystallite size of the ZT pigment is 91nm.

S2 Supplemental Experimental Procedure S2:Characterization of SEM and EDS

SEM measurements were performed to observe the morphological features of the synthesized pigments, shown in Fig. S2. It can be found that the pure $ZnTiO_3$ pigment has a weakly agglomerated near-flaky particle composition. The particle size of all compositions varies from 20 to 150 nm.

To study the elemental composition and distribution, the $ZnTiO_3$ pigment was further carried out by EDS and elemental mapping, as shown in Fig. S2. The EDS results of $ZnTiO_3$ (Fig. 5a) verified the presence of Zn, Ti, and O elements in the pigment structure, which corresponds to the

XPS results. According to the element content analysis results obtained by EDS, the molar ratio of Zn and Ti is consistent with the stoichiometry of $ZnTiO_3$. Furthermore, the elemental mapping images indicated a uniform distribution of the three elements in the pigment (Fig. S2 e–f).

S3 Supplemental Experimental Procedure S3:Characterization of XPS

XPS measurements were performed on perovskite $ZnTiO_3$ nanoparticles to determine the surface composition and chemical state. The obtained spectrum is shown in Figure 5. Strong peaks corresponding to the O1s, Zn2p, and Ti2p core levels were seen in XPS survey scans. The Zn peaks' binding energies are 1021.4 eV and 1044.5 eV, respectively, and are attributed to $Zn2p_{3/2}$ and $Zn2p_{1/2}$.[2]. $Ti2p_{3/2}$ and $Ti2p_{1/2}$ are responsible for the doublet's peaks at 458.4 eV and 464.2 eV, respectively. It denotes the Ti ion's tetravalent state. [3, 4]. The O 1s XPS peak is shown in Fig. 3(d), along with the best fitted data. Two peaks with centers at 529.9 and 531.6 eV, respectively, represent the divalent state of oxygen (O^{2-}) and chemisorbed oxygen.

S4 Supplemental Experimental Procedure S4:Characterization of Chemical Shielding Test

Fig S4(a) illustrates the chemical resistance of coatings to salt solution, strong acid solution, and strong alkali solution.. Droplets of the aforementioned solution (0.5 mL) were applied to the polished semi-coated tinplate for 0, 24, and 96 hours, respectively. Contact angles of the coating surface to 5.0 wt % NaCl solution, saturated $Ca(OH)_2$ solution and 5 wt% H_2SO_4 solutions can be found in figure S4(b). The contact angle of the coating was measured before and after the chemical shielding test. By comparison, it was found that the change of the contact angle was very small, indicating that the chemical shielding ability of the coating was very strong.

Supplemental Figures

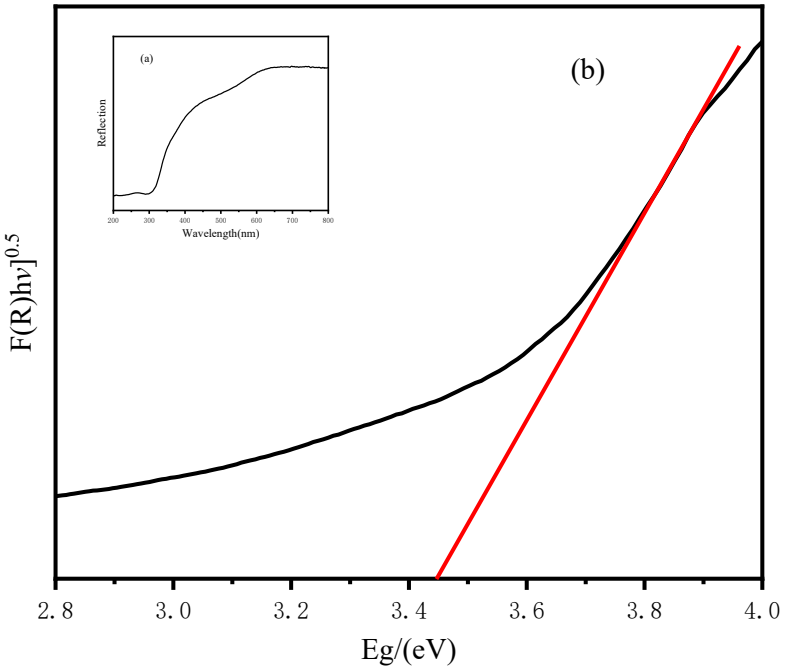

Figure S1. The band gap of ZT

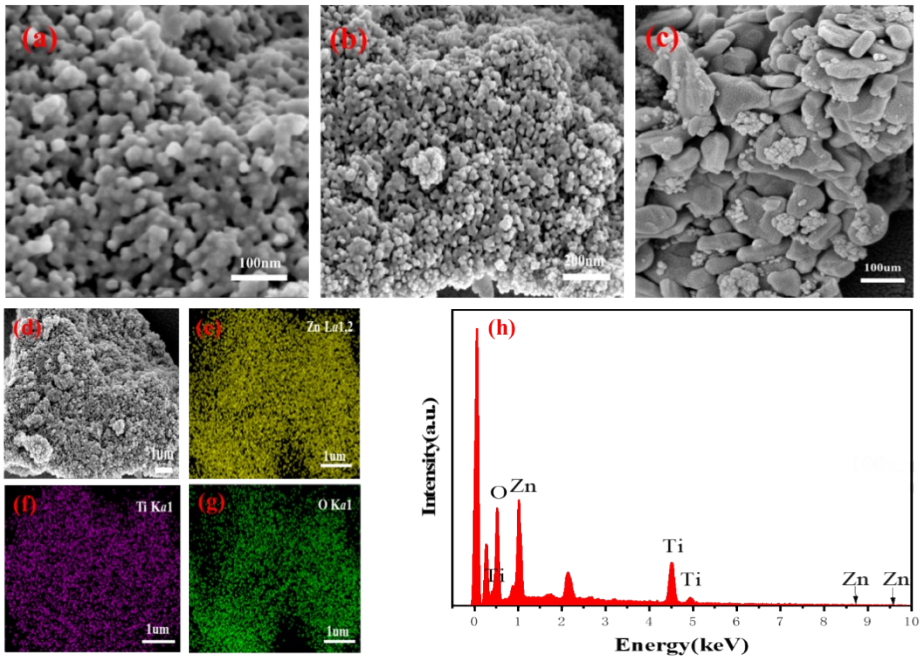

Figure S2. SEM images of (a, b) ZT, (b−f) elemental mapping, and EDS of ZT.

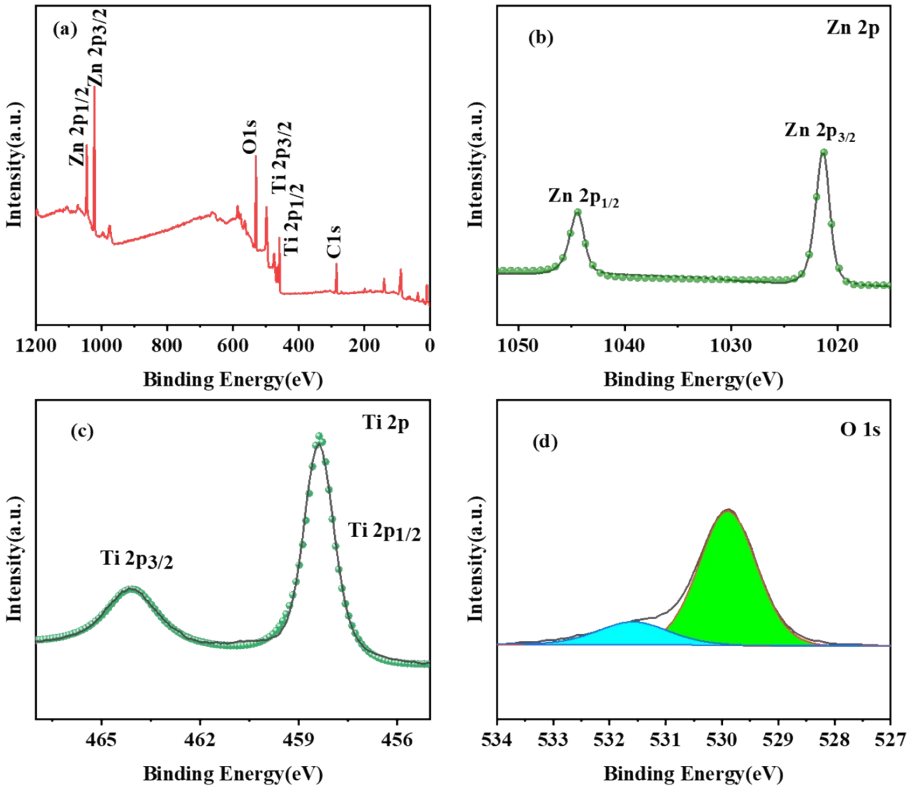

Figure S3. XPS of ZT sample (a) full survey, (b) Zn 2p, (c) Ti 2p, and (d) O 1s.

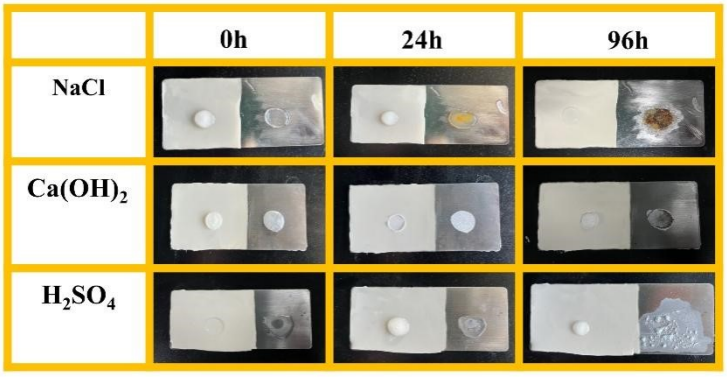

Figure S4a Chemical shielding ability of M-ZT composite coatings.

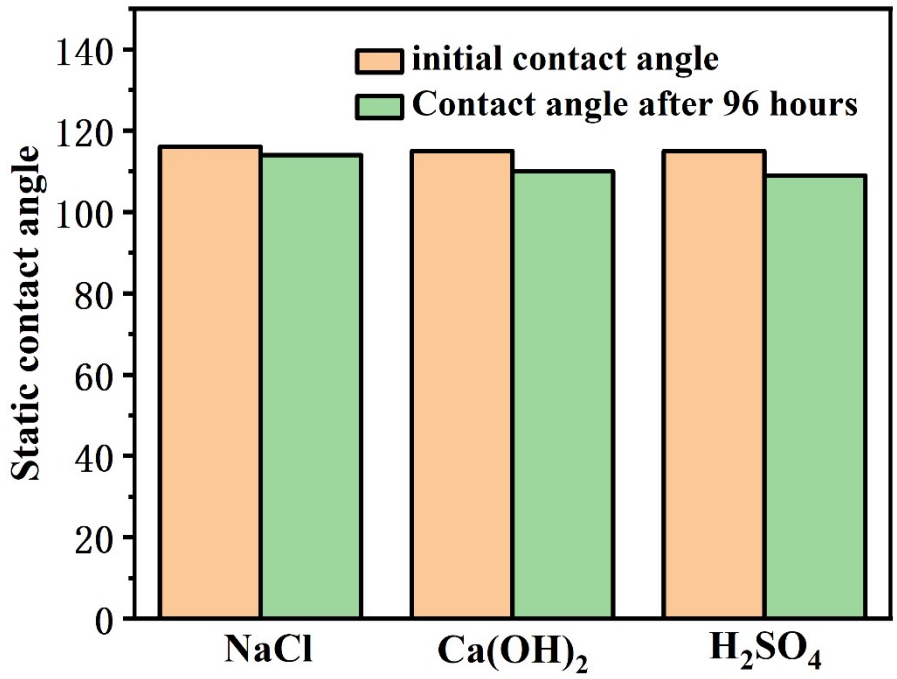

Figure S4b The contact angle of M-ZT composite coatings before and after the chemical shielding

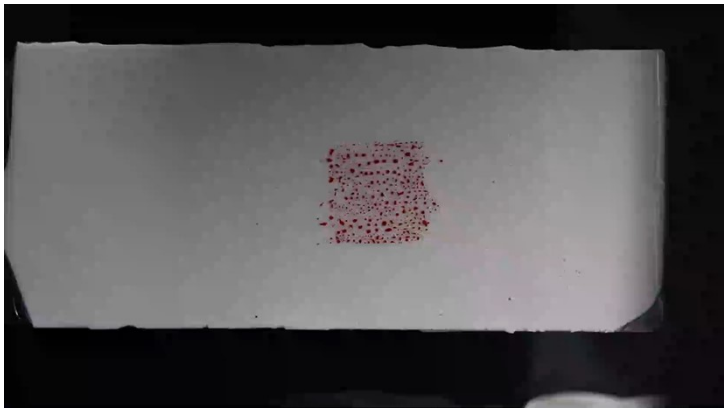

Movie S1 Removal of oily red marker.

Movie S2 Removal of graffiti with water-based ink

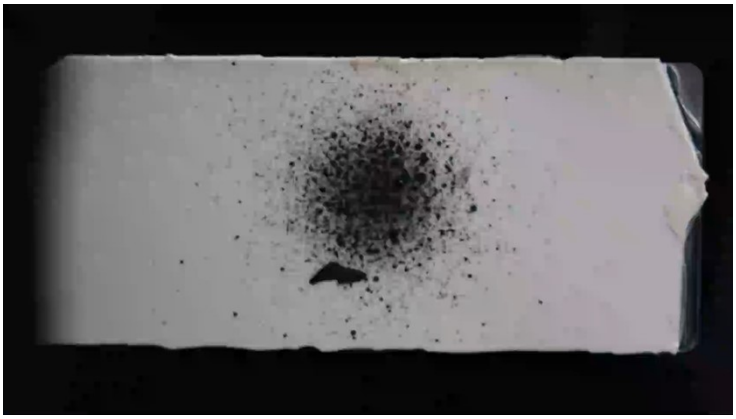

Movie S3 Removal of graffiti with paint.

[1] W. Zhou, Y. Liu, Q. Sun, J. Ye, L. Chen, J. Wang, G. Li, H. Lin, Y. Ye, W. Chen, High Near-Infrared Reflectance Orange Pigments of Fe-Doped La2W2O9: Preparation, Characterization, and Energy Consumption Simulation, ACS Sustainable Chemistry & Engineering 9(36) (2021) 12385-12393.
[2] R. Al-Gaashani, S. Radiman, A.R. Daud, N. Tabet, Y. Al-Douri, XPS and optical studies of different morphologies of ZnO nanostructures prepared by microwave methods, Ceramics International 39(3)

(2013) 2283-2292.
[3] I.R. Galindo, T. Viveros, D. Chadwick, Synthesis and Characterization of Titania-Based Ternary and Binary Mixed Oxides Prepared by the Sol−Gel Method and Their Activity in 2-Propanol Dehydration, Industrial & Engineering Chemistry Research 46(4) (2007) 1138-1147.
[4] G.L. Bhagyalekshmi, A.P. Neethu Sha, D.N. Rajendran, Luminescence kinetics of low temperature nano ZnTiO3:Eu3+ red spinel under NUV excitation, Journal of Materials Science: Materials in Electronics 30(11) (2019) 10673-10685.
[5] Y.J. Kang, D.S. Kim, S.H. Lee, J. Park, J. Chang, J.Y. Moon, G. Lee, J. Yoon, Y. Jo, M.-H. Jung, Ferromagnetic Zn1-xMnxO (x = 0.05, 0.1, and 0.2) Nanowires, The Journal of Physical Chemistry C 111(41) (2007) 14956-14961.